NASA Technical Memorandum 103120
AIAA-90-2271

Performance Characteristics of a One-Third-Scale, Vectorable Ventral Nozzle for SSTOVL Aircraft

Barbara S. Esker and Jack G. McArdle
Lewis Research Center
Cleveland, Ohio

Prepared for the
26th Joint Propulsion Conference
cosponsored by the AIAA, ASME, SAE, and ASEE
Orlando, Florida, July 16-18, 1990

NASA

PERFORMANCE CHARACTERISTICS OF A ONE-THIRD-SCALE, VECTORABLE VENTRAL NOZZLE FOR SSTOVL AIRCRAFT

Barbara S. Esker and Jack G. McArdle
National Aeronautics and Space Administration
Lewis Research Center
Cleveland, Ohio 44135

Abstract

Several proposed configurations for possible supersonic short-takeoff, vertical-landing (SSTOVL) aircraft will require a ventral nozzle in the lower fuselage for lift and pitch control. The swivel nozzle is one possible ventral nozzle configuration. At NASA Lewis Research Center an approximately one-third-scale swivel nozzle model was built and tested on an existing generic model tailpipe with the exhaust closed. This particular swivel nozzle configuration is designed to vector the ventral flow up to ±23° from the vertical position. The ventral duct had square edges where it intersected the tailpipe. Steady-state performance data were obtained for pressure ratios to 4.5, and pitot-pressure surveys were made at the nozzle exit plane. Thrust measurements indicated that the effective flow angle was consistently 5° more than the set nozzle vector angle. This flow angle resulted from a low-pressure region along the upstream wall of the ventral duct and swivel nozzle, a phenomenon that can be seen in the pitot-pressure contours of the nozzle exit plane. The swivel nozzle was further studied to determine the change in performance resulting from rounding the contour of the leading edge of the ventral duct inlet. This modification increased the nozzle discharge coefficient, reduced the severity of the low-pressure region along the upstream wall, and reduced the difference between the effective flow angle and the set vector angle of the nozzle.

Introduction

Supersonic short-takeoff, vertical-landing (SSTOVL) aircraft concepts are potential candidates for future fighter applications. Several SSTOVL aircraft[1] would use a single propulsion system to provide power for both lift and hover as well as supersonic horizontal flight. Studies indicate that propulsion technologies are the key to developing successful SSTOVL aircraft designs, and NASA Lewis Research Center is addressing this important point.

Possible propulsion configurations for these aircraft include mixed-flow vectored thrust, tandem fan, lift plus lift cruise, ejector, and the remote augmented lift system (RALS). Artists' renditions of aircraft using these propulsion systems are shown in Fig. 1. Other propulsion concepts, such as lift fans, are not shown. All of these propulsion configurations could use a ventral nozzle for lift and pitch control. The ventral nozzle would be located in the lower fuselage of the aircraft, aft of the center of gravity. When lift is required, a valve would open the engine tailpipe to the ventral duct, directing a jet of mixed exhaust gases downward. During hover the main exhaust nozzle would be closed, and the ventral nozzle and other lift-producing devices would be activated.

A rectangular swivel nozzle (Fig. 2) is a particular ventral nozzle design capable of vectoring the downward flow for lift and pitch control. Vectoring is accomplished by an outer shell that pivots about an axis perpendicular to both the tailpipe axis and the ventral nozzle axis. In this design the shell can pivot 23° on either side of the midposition. This uncomplicated configuration can vector the flow with only a few moving parts and could be easily actuated with minimal sealing problems. If required, variable exit area could be achieved by independently actuating the halves of the outer shell.

In order to determine the performance characteristics of this type of nozzle, a one-third-scale swivel nozzle was built and tested on the NASA Lewis Research Center's Powered Lift Facility (PLF). The PLF is an outdoor test stand with a six-component force-measuring system. The major test objectives were to measure the thrust and internal flow performance parameters for the nozzle over the vectoring range. Two configurations were tested: the swivel nozzle with a square contour of the leading edge of the ventral duct inlet and the same nozzle with a round leading-edge contour. This comparison was of interest because previous work with ventral nozzles[2] showed that large turning losses are incurred with the square leading-edge contour. The tests measured steady-state performance at ratios of tailpipe to ambient pressure to 4.5 for vector angle settings of 70°, 80°, 90° (midposition), 100°, and 110° from the exhaust axis. A survey of pitot pressures at the nozzle exit plane was made at a tailpipe pressure ratio of 3.0 for the 90° setting. Wall static-pressure measurements were made in the nozzle shell to study the airflow velocity and pressure loads in the nozzle. The results are shown in plots of discharge coefficient, thrust coefficient, and other important performance data for the various configurations. The changes brought about by rounding the contour of the leading (or upstream) edge of the ventral duct inlet are noted. Pitot-pressure distributions are shown in contour plots of the nozzle exit plane for both the square- and round-leading-edge configurations.

Apparatus and Instrumentation

Model

The model swivel nozzle (Fig. 2) is conceptually the same as a round model tested many years ago.[3] For the present nozzle the exit geometry is 4.6 in. by 13.5 in., approximately one-third of full size. Figure 2(a) shows the swivel nozzle in the midposition (90°). Vectoring can be achieved by "swiveling" or pivoting the outer shell. The outer shell can be pivoted up to 23° on either side of the midposition. Figure 2(b) shows the swivel nozzle in one of the fully pivoted positions.

(a) EJECTOR AUGMENTOR.

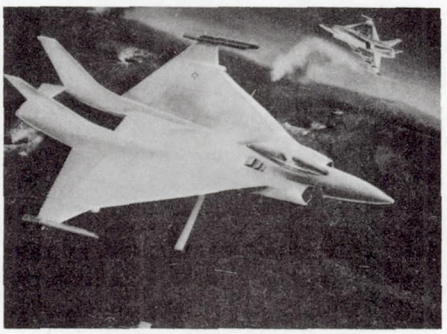

(b) REMOTE AUGMENTED LIFT SYSTEM.

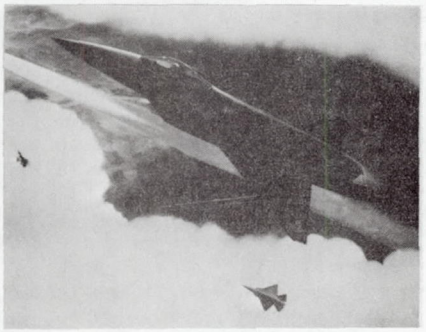

(c) MIXED-FLOW VECTORED THRUST.

(d) HYBRID TANDEM FAN.

FIG. 1. ARTISTS' CONCEPTIONS OF POSSIBLE CONFIGURATIONS FOR FUTURE SUPERSONIC STOVL AIRCRAFT.

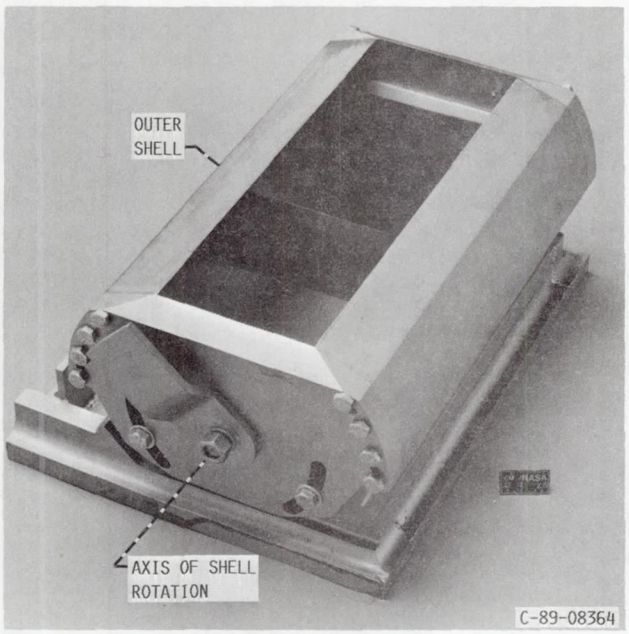

(a) IN MIDPOSITION.

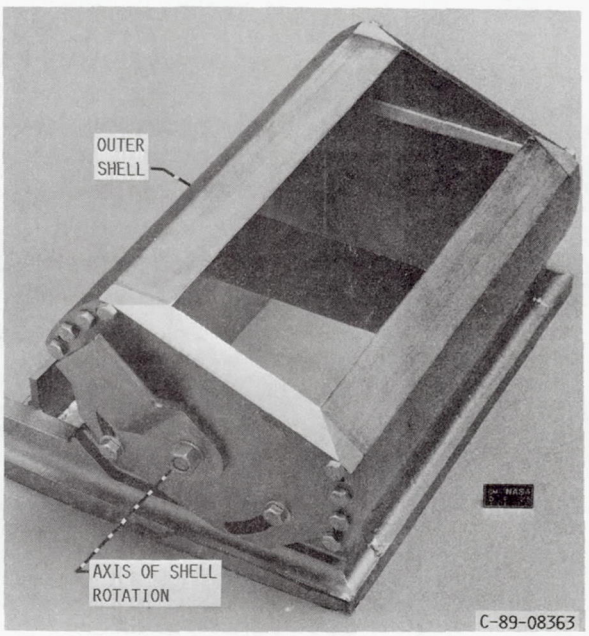

(b) IN ROTATED POSITION.

FIG. 2. SWIVEL NOZZLE.

In the test program the swivel nozzle was mounted on an existing one-third-scale tailpipe model. A sketch of the tailpipe with the swivel nozzle is shown in Fig. 3. The tailpipe was mounted on a facility transition section made up of two honeycomb flow straighteners and a fine-mesh screen to smooth the inflow. A boundary layer trip was used to ensure a turbulent boundary layer. The free-stream turbulence intensity was not measured for the present tests, but from previous results[4] it was expected to be less than 0.5 percent. The end of the tailpipe was closed off with a blind flange to simulate a blocked exhaust nozzle. An adapter block, made of synthetic wood and shown in Figs. 3 and 4, was used to reduce the original ventral duct opening to the size needed for the swivel nozzle. The block (Fig. 4) was first machined to have a square contour to provide a square leading edge for the ventral duct inlet. In the later modification the block was machined to a round contour to provide a round leading edge for the ventral duct inlet. The radius of the contour at the centerline was equal to the thickness of the block. This radius tapered smoothly to zero at the outer sides.

Stand

The tailpipe and swivel nozzle configuration was mounted on the PLF as shown in Fig. 5. This outdoor test stand can measure three forces (axial, normal, and side) and three moments (pitch, roll, and yaw). Thrust and lift forces were computed from these measurements. The effective flow angle was calculated from the thrust and lift forces. The capability of the stand to accurately measure the forces and compute the effective flow angle was established by using a standard nozzle and precise pipe elbows to produce a flow at a known angle. The effective flow angle was found to be equal to the known flow angle to within ±1°. Airflow measurements for the PLF were made with an ASME nozzle in the facility air supply line.

Instrumentation

Instrumentation for the swivel nozzle test is shown in Fig. 6, a photograph of the tailpipe and the nozzle. Wall static-pressure measurements were made in the tailpipe, the ventral duct, and the swivel nozzle. Tailpipe total-pressure measurements were made with four rakes each having five total-pressure probes on centers of equal areas. These measurements were made at station 5 (Fig. 3) upstream of the ventral duct, allowing the performance of the swivel nozzle to be referenced to the tailpipe conditions. Ventral duct total-pressure measurements were made with 24 probes spaced uniformly at station 6 (Fig. 3), allowing the performance of the nozzle to be referenced to the nozzle inlet conditions. A five-tip total-pressure rake was designed and built for a pitot-pressure survey of the nozzle exit plane (station 6B, Fig. 3). The complete hardware, including the rake, the actuator, and the motor, is shown mounted to the tailpipe and the swivel nozzle in Fig. 7. Data were recorded on the Center's data acquisition system. Extensive computations were made on the VAX computer system.

Testing Procedure

Steady-state performance testing of the swivel nozzle consisted of flow and thrust measurements at tailpipe pressure ratios to 4.5. Airflow was controlled by a valve in the facility air supply line. Tests were done for swivel nozzle vector angle settings of 70°, 80°, 90° (midposition), 100°, and 110° (Fig. 8).

Pitot-pressure surveys were made at the nozzle exit (station 6B, Fig. 3). For this part of the test the five-tip rake was traversed across a plane 0.25 in. downstream of the nozzle exit.

Results and Discussion

In this discussion the performance characteristics are defined as follows:

(1) Discharge coefficient, C_d, the measured flow rate divided by the ideal flow rate at the same tailpipe conditions and pressure ratio

(2) Total thrust coefficient, C_f, the measured total thrust divided by the ideal thrust produced by the measured flow at the same tailpipe conditions and pressure ratio

Square-Leading-Edge Configuration

Discharge coefficient. The flow characteristics of the swivel nozzle (Fig. 9) were found to vary with the vector angle setting and the pressure ratio. The highest discharge coefficient occurred with the swivel nozzle vector angle set at 110° (C_d = 0.874 for a tailpipe pressure ratio of 3.0). In contrast, the lowest discharge coefficient occurred with the vector angle set at 70° (C_d = 0.854 for a tailpipe pressure ratio of 3.0). Generalizing, the discharge coefficient increased as the flow was vectored back toward the model inlet. Previous work[2] has shown that the flow turns more than 90° in the ventral duct. This occurs because the flow separates from the upstream wall (Fig. 8) after passing over the square leading edge of the ventral opening, making the pressure less on the upstream wall than on the downstream wall. This pressure difference causes the main flow to continue to turn as it passes through the ventral duct. It follows, then, that the discharge coefficient is higher when the flow is allowed to continue overturning through the swivel nozzle (i.e., when the vector angle setting is greater than 90°).

Thrust coefficient. Unlike the discharge coefficient, the thrust coefficient (Fig. 10) was not significantly affected by the swivel nozzle vector angle setting (except at 70°). Overall, the thrust coefficient reached a steady-state value of approximately 0.97 at a tailpipe pressure ratio of 3.0.

Horizontal thrust component and effective flow angle. Figure 11 shows a plot of the horizontal thrust versus the vector angle setting. A negative horizontal thrust existed when the nozzle was set at a 90° vector angle. This indicates that the flow had been exiting the nozzle at an effective flow angle greater than the vector angle setting. At a 110° vector angle a larger negative thrust existed than was expected if the effective flow angle were equal to the vector angle setting. Similarly, at a 70° vector angle, a smaller positive horizontal thrust existed.

The negative horizontal thrust component described in the preceding paragraph was a result of an overall "offset" between the vector angle

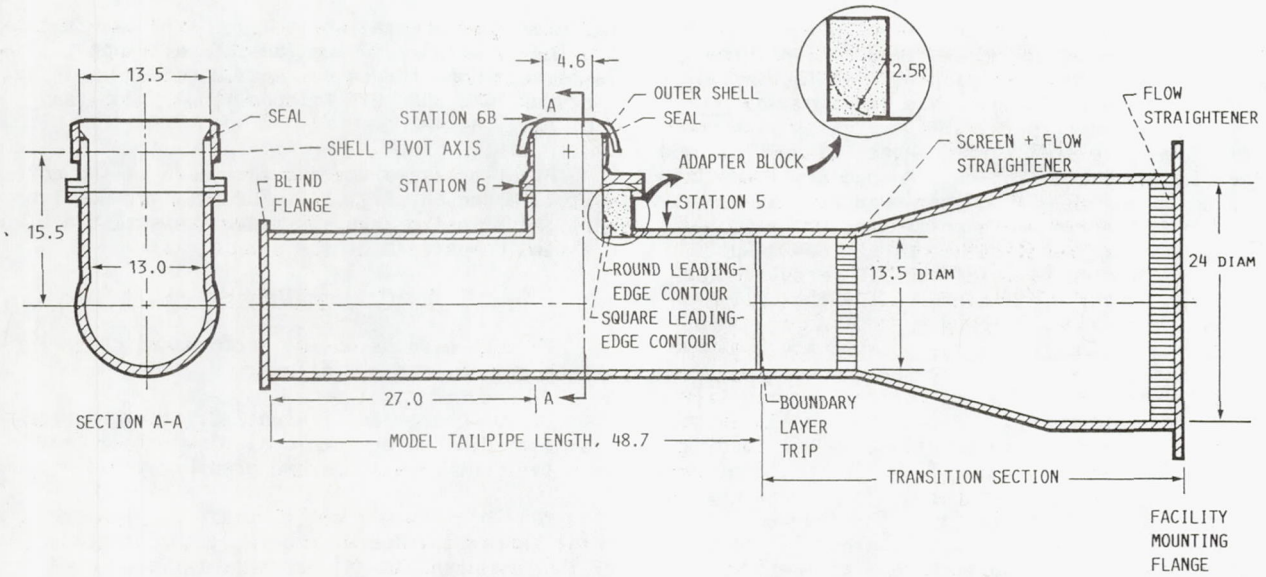

FIG. 3. CROSS SECTION OF SWIVEL NOZZLE AND TAILPIPE ASSEMBLY. (DIMENSIONS ARE IN INCHES.)

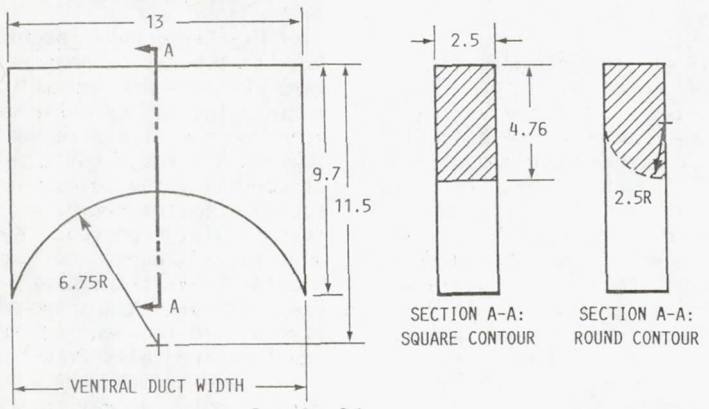

FIG. 4. ADAPTER BLOCK. (DIMENSIONS ARE IN INCHES.)

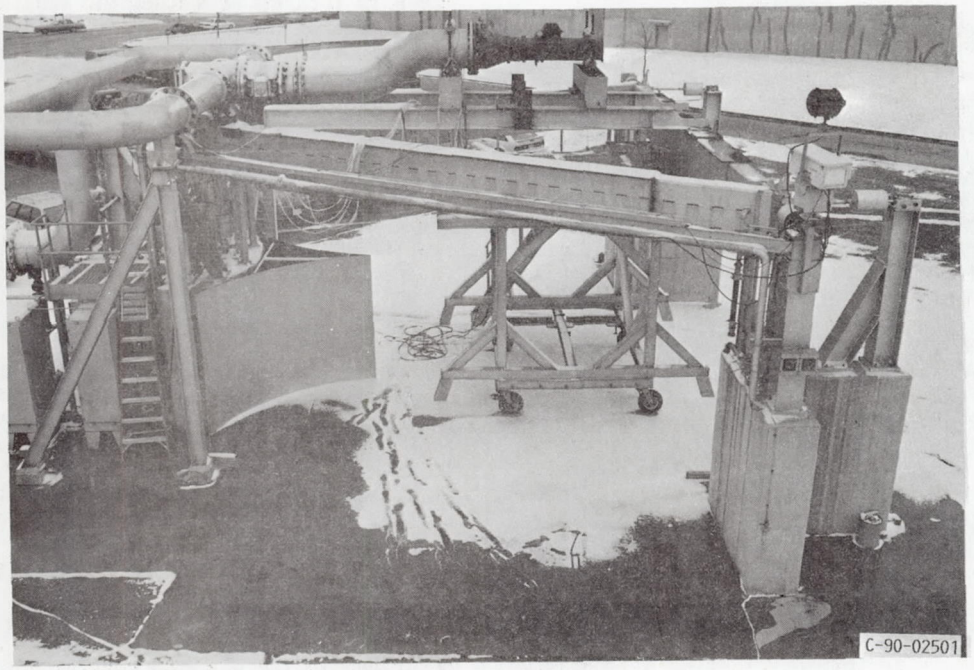

FIG. 5. POWERED LIFT FACILITY WITH TAILPIPE.

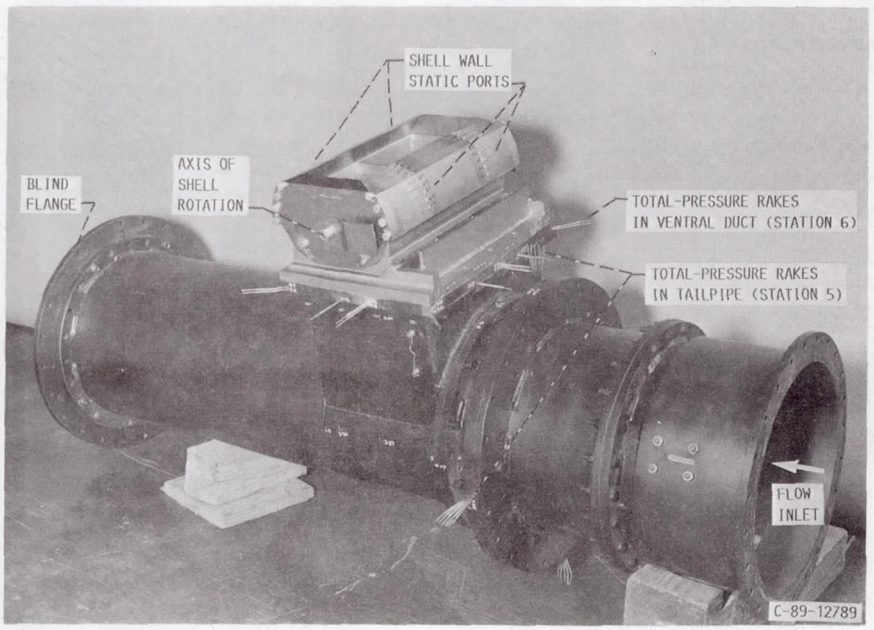

FIG. 6. SWIVEL NOZZLE ON TAILPIPE WITH INSTRUMENTATION.

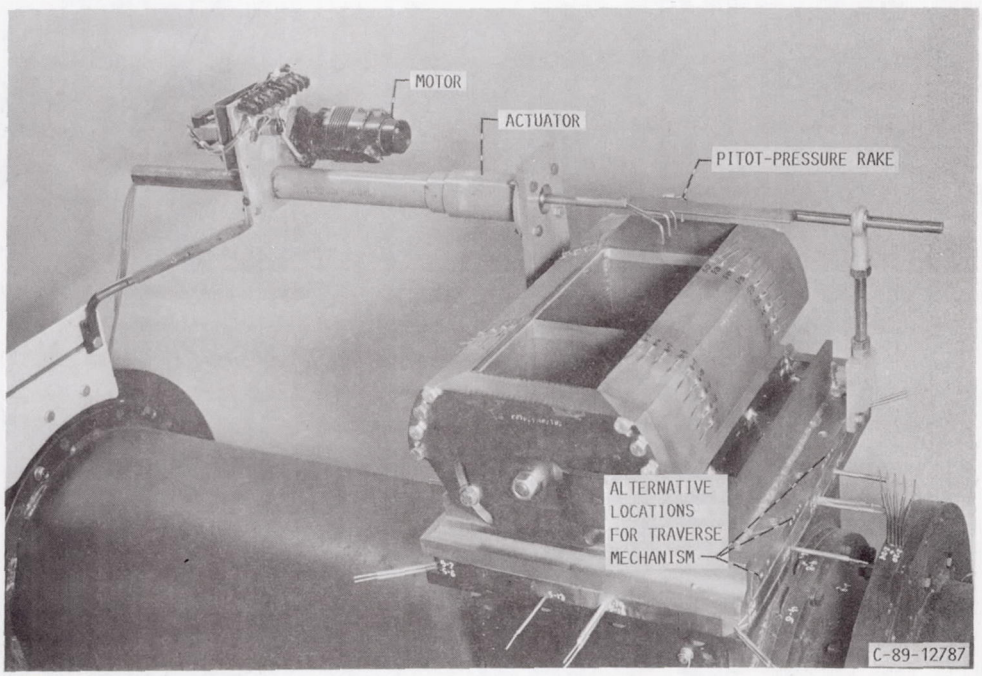

FIG. 7. PITOT-PRESSURE TRAVERSE INSTRUMENTATION.

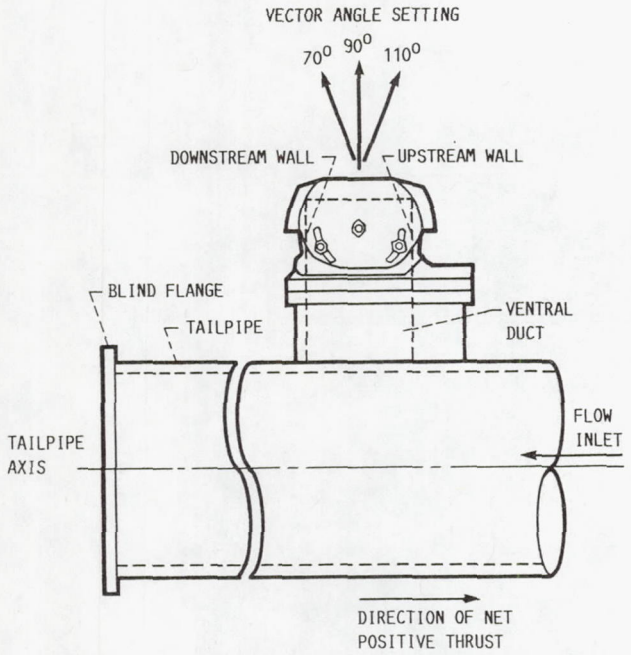

FIG. 8. SWIVEL NOZZLE AND TAILPIPE ASSEMBLY.

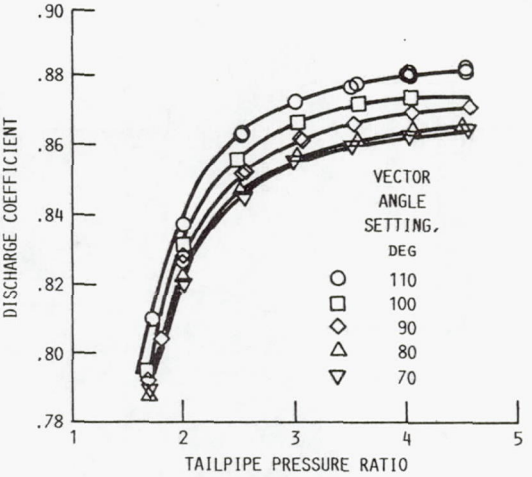

FIG. 9. VARIATION OF DISCHARGE COEFFICIENT WITH TAILPIPE PRESSURE RATIO FOR SQUARE-LEADING-EDGE CONFIGURATION.

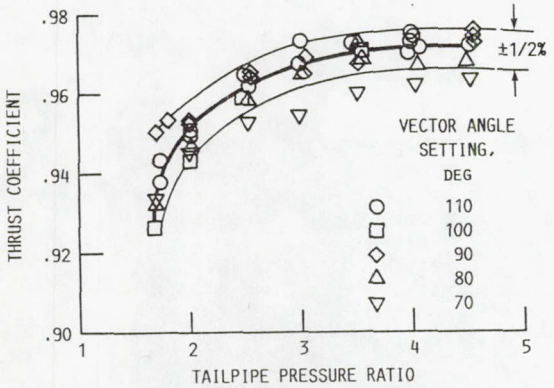

FIG. 10. VARIATION OF THRUST COEFFICIENT WITH TAILPIPE PRESSURE RATIO FOR SQUARE-LEADING-EDGE CONFIGURATION.

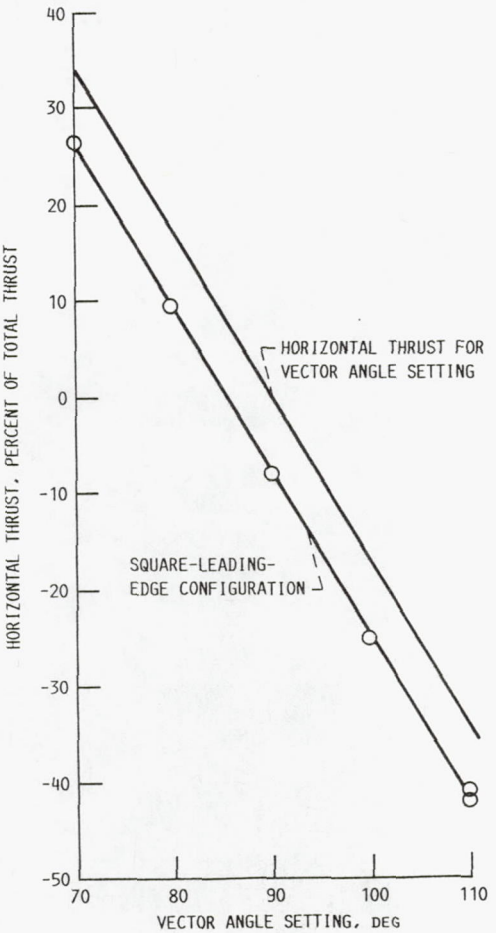

FIG. 11. VARIATION OF HORIZONTAL THRUST WITH VECTOR ANGLE SETTING FOR SQUARE-LEADING-EDGE CONFIGURATION.

setting and the effective flow angle, shown clearly in Fig. 12. This offset was constant and independent of the vector angle setting, and its value was 5° at a tailpipe pressure ratio of 3.0.

Figure 13 shows the effect of the tailpipe pressure ratio on the effective flow angle for a 90° vector angle. As the pressure ratio increased, the effective flow angle decreased slightly, causing a reduced offset at high pressure ratios. The same effect also occurred for the other vector angles settings.

Exit pressure survey. A contour plot of pitot pressures at the nozzle exit plane is shown in Fig. 14. The values were obtained from the pitot-pressure survey. The five-probe rake was traversed at a constant normalized tailpipe pressure ratio of 3.0. The flow was symmetric laterally. A region of low pressure existed along the upstream wall of the nozzle. In this region pitot pressure dropped from 92 percent to 85 percent of the tailpipe total pressure. Previous testing with a convergent ventral nozzle[2] indicated that flow from the aft half of the ventral nozzle moves forward toward the upstream wall because of this low-pressure region. The resultant exit flow angle caused the net negative horizontal thrust component. The maximum pressure (99.8 percent of tailpipe pressure) occurred in small regions on either side of the nozzle that were located in the aft half of the nozzle exit area.

Round-Leading-Edge Configuration

The testing of the swivel nozzle also included an investigation of a round (more aerodynamic) contour for the leading edge of the ventral duct inlet and its effect on the performance of the swivel nozzle. The modification made to the leading edge is shown in Figs. 3 and 4. Note that only the leading edge of the ventral duct was rounded; the remaining three duct edges were not modified. The modified leading edge was intended to reduce turning losses into the ventral duct and thus improve the performance of the ventral system.

Turning losses. The round-contour leading edge was successful in reducing the turning losses (losses that occur from the flow turning into the ventral duct). This result is shown graphically in Fig. 15. The square-leading-edge configuration exhibited turning losses of 6 percent. In contrast, the round-leading-edge configuration showed losses of less than 1.4 percent.

Discharge coefficient. Further benefits from the round-contour leading edge are shown in Fig. 16. The discharge coefficient increased significantly as a result of this modification. Figure 16 shows the discharge coefficient for the swivel nozzle set at a 90° vector angle. This parameter increased from 0.87 for the square-leading-edge configuration to 0.91 for the round-leading-edge configuration. The same result was found for the other vector angles tested.

Thrust coefficient. Figure 17 shows the variation of the thrust coefficient with the tailpipe pressure ratio for the round-leading-edge configuration. As with the square-leading-edge configuration, the thrust coefficient was unaffected by the nozzle vector angle setting, but it was slightly greater than that measured for the square-leading-edge configuration. This difference was more pronounced at lower tailpipe pressure ratios.

Horizontal thrust component and effective flow angle. Figure 18 shows the horizontal thrust over the range of vector angles settings for both the square- and round-leading-edge configurations. At a 90° vector angle the negative thrust for the round-edge configuration was less in magnitude than the negative thrust for the square-edge configuration. The negative horizontal thrust component was a result of the flow exiting at an angle greater than the vector angle setting. Figure 19 shows the effective flow angle plotted against the vector angle setting for both configurations. Also shown in Fig. 19 is a theoretical result if the effective flow angle were equal to the vector angle setting. The effect of the round leading edge was a decrease in the difference between the effective flow angle and the theoretical result. The difference decreased from 5° for the square-leading-edge configuration to 2.5° for the round-leading-edge configuration. This implies that the region of low pressure along the upstream wall had been reduced in size and strength. This low-pressure region was the cause of the offset between the vector angle setting and the effective flow angle. A contour plot of the pitot pressures at the nozzle exit plane explicitly shows the reduction of the low-pressure region. This will be presented in a following figure.

Figure 20 shows the effect of the tailpipe pressure ratio on the effective flow angle for the round-edge configuration at a 90° vector angle. With the round edge, as with the square edge, the difference between the vector angle setting and the effective flow angle decreased with an increase in tailpipe pressure ratio. This figure gives an offset of approximately 2.3° at low pressure ratios and approximately 1.3° at high pressure ratios. Similar results were obtained for other vector angle settings.

Exit pressure survey. As mentioned previously, the reduced negative horizontal thrust for the round-leading-edge configuration implied that the low-pressure region along the upstream wall had changed. Figure 21 shows the contour plot of the pitot pressures at the nozzle exit plane. The low-pressure region showed a minimum of 92 percent of total upstream tailpipe pressure. In contrast, Fig. 14 shows a contour plot for the square-leading-edge configuration, the minimum pressure being 85 percent of the total upstream tailpipe pressure. Also, the area of the low-pressure region is smaller with the round edge (Fig. 21).

Shell wall pressures. In Fig. 22 the ratio of measured shell wall pressure to tailpipe total pressure is plotted against the ratio of nozzle cross-sectional flow area to nozzle exit area. The one-dimensional isentropic pressure ratio is also shown for two cases: (1) the ideal flow case, where the flow area is equal to the geometric exit area, and (2) the measured flow case, where the flow area is equal to the geometric exit area times the measured discharge coefficient. For the square-leading-edge configuration the wall pressures were higher on the rear shell surface than on the front shell surface. This indicates that the

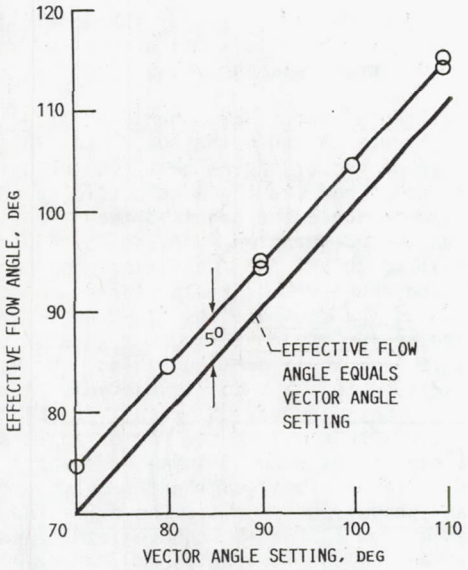

FIG. 12. VARIATION OF EFFECTIVE FLOW ANGLE WITH VECTOR ANGLE SETTING FOR SQUARE-LEADING-EDGE CONFIGURATION. TAILPIPE PRESSURE RATIO, 3.0.

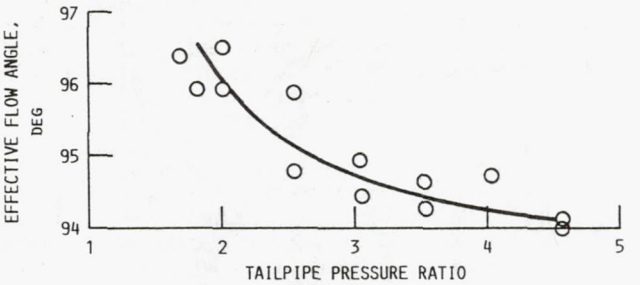

FIG. 13. VARIATION OF EFFECTIVE FLOW ANGLE WITH TAILPIPE PRESSURE RATIO FOR SQUARE-LEADING-EDGE CONFIGURATION. VECTOR ANGLE SETTING, 90°.

CONTOUR	PRESSURE, PERCENT OF TAILPIPE TOTAL PRESSURE
A	60
B	80
C	85
D	89
E	92
F	94
G	98.5
H	99.2
I	99.8

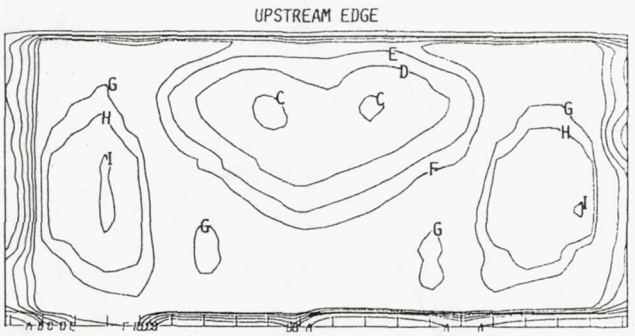

FIG. 14 CONTOUR PLOT OF PITOT PRESSURES AT SWIVEL NOZZLE EXIT (STATION 6B) FOR SQUARE-LEADING-EDGE CONFIGURATION. NORMALIZED TAILPIPE PRESSURE RATIO, 3.0. (AIRFLOW COMING OUT OF PAGE.)

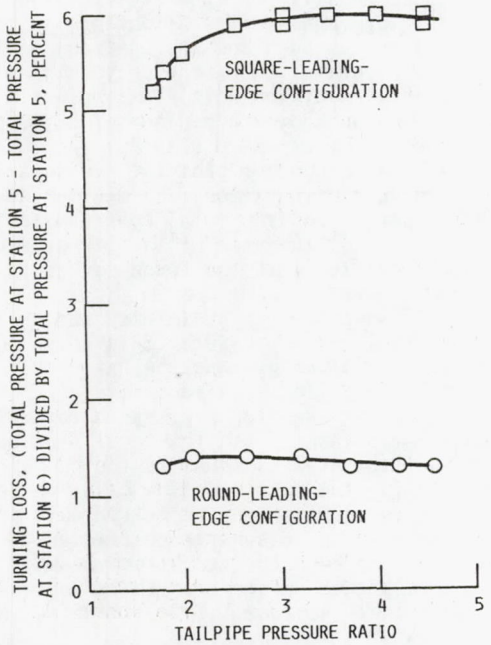

FIG. 15. FLOW TURNING LOSS FOR BOTH CONFIGURATIONS.

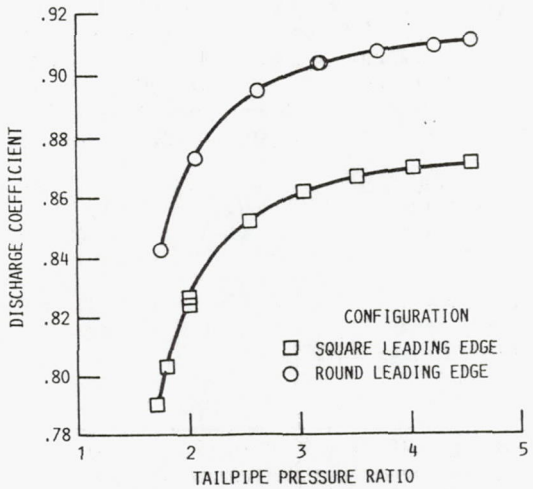

FIG. 16. COMPARISON OF DISCHARGE COEFFICIENTS FOR BOTH CONFIGURATIONS. VECTOR ANGLE SETTING, 90°.

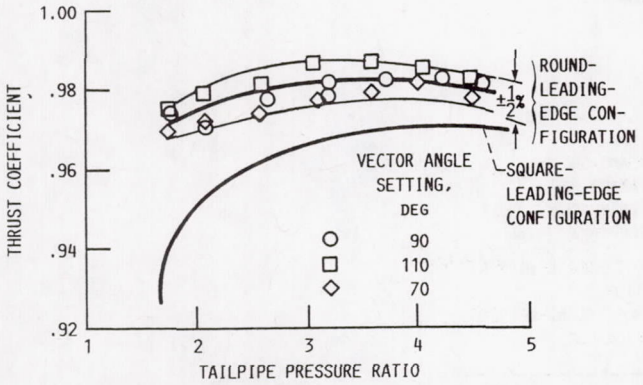

FIG. 17. COMPARISON OF THRUST COEFFICIENTS FOR BOTH CONFIGURATIONS.

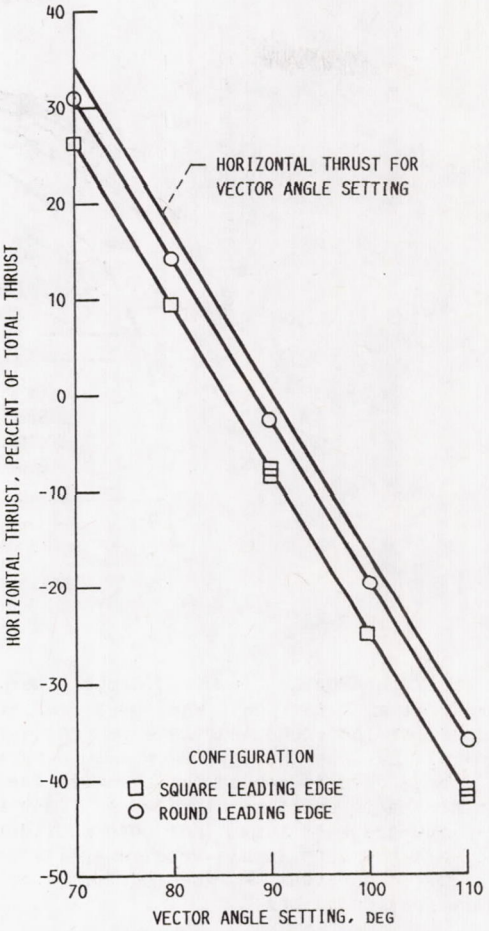

FIG. 18. COMPARISON OF HORIZONTAL THRUST FOR BOTH CONFIGURATIONS.

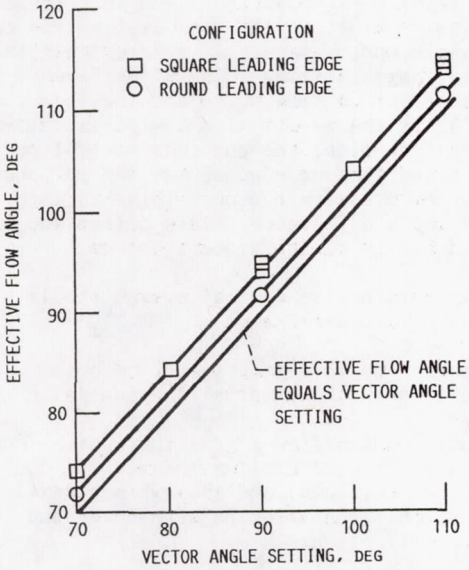

FIG. 19. VARIATION OF EFFECTIVE FLOW ANGLE WITH VECTOR ANGLE SETTING FOR BOTH CONFIGURATIONS.

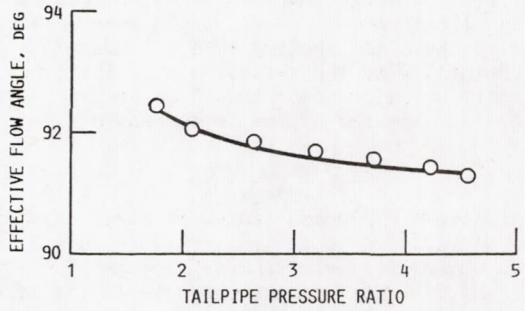

FIG. 20. VARIATION OF EFFECTIVE FLOW ANGLE WITH TAILPIPE PRESSURE RATIO FOR ROUND-LEADING-EDGE CONFIGURATION. VECTOR ANGLE SETTING, 90^{o}.

CONTOUR	PRESSURE, PERCENT OF TAILPIPE TOTAL PRESSURE
A	60
B	80
C	85
D	89
E	92
F	94
G	98.5
H	99.2
I	99.8

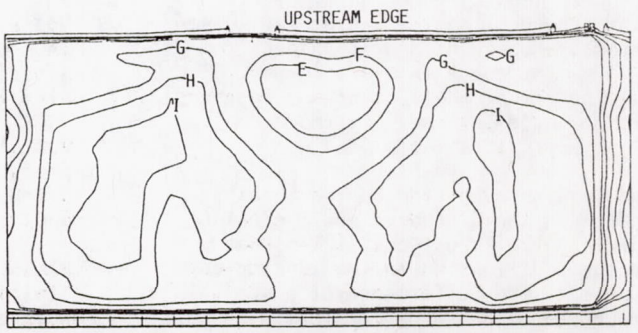

FIG. 21 CONTOUR PLOT OF PITOT PRESSURES AT SWIVEL NOZZLE EXIT FOR ROUND-LEADING-EDGE CONFIGURATION. NORMALIZED TAILPIPE PRESSURE RATIO, 3.0. (AIRFLOW COMING OUT OF PAGE.)

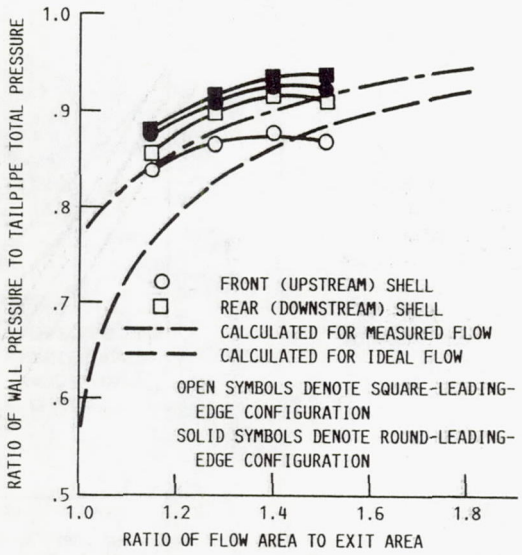

FIG. 22. SHELL WALL PRESSURES. TAILPIPE PRESSURE RATIO, 3.0; VECTOR ANGLE SETTING, 90^{o}.

flow was still turning as it moved through the nozzle. The front and rear shell wall pressures were almost equal for the round-leading-edge configuration, showing that the throughflow was more nearly uniform. These results are compatible with the trends in discharge coefficient, flow exit angle, and exit-plane pressure maps. For both configurations the wall-pressure levels were generally as high or higher than might be expected from simple flow theory considerations.

The shell structure must be strong enough to withstand the pressure loads without structural distortion that might cause binding or reduced sealing effectiveness. Shell hinge moments are minimal because the shell pressure loads are reacted totally by the swivel joint. Therefore, only small actuator power should be needed to vary the nozzle exit area or the vector angle.

Concluding Remarks

A swivel nozzle was tested at steady-state ratios of tailpipe to ambient pressure to 4.5. The two objectives were successfully met: (1) the thrust and flow performance characteristics were measured. (2) a change in these characteristics resulted from changing the contour of the leading edge of the ventral duct inlet from a square to a round edge.

For the square leading edge the discharge coefficient was dependent on the vector angle setting. At a pressure ratio of 3.0 it ranged from 0.854 for a 70° vector angle to 0.874 for a 110° vector angle. The thrust coefficient was independent of the vector angle setting. It reached a value of 0.97 at a pressure ratio of 3.0.

The round leading edge reduced the turning losses and increased the discharge coefficient of the swivel nozzle. The thrust coefficient was unaffected by the modification to the leading edge. In order to maximize the performance of a ventral nozzle, the round edge should be considered as part of the ventral system design.

The presence of a negative horizontal thrust at a vector angle setting of 90° is important. For the square-leading-edge configuration this thrust component was a result of the flow exiting the nozzle at an angle approximately 5° greater than the nozzle vector angle setting. The 5° difference between the effective flow angle and the vector angle setting is the result of a low-pressure region of separated flow along the upstream ventral duct wall. The round leading edge of the ventral duct reduced the low-pressure region. This. in turn, reduced the angle difference. This offset should be accounted for in flight systems design.

Many aspects of the ventral system should be considered for future research:

(1) Ventral duct length, shape, or both
(2) Tailpipe Mach number at the ventral duct inlet
(3) Additional offtakes near the ventral duct
(4) Design of controls for the ventral duct or offtakes (or both) and the exhaust nozzle during the transition between hover and horizontal flight

References

1. Levine, J. and Inglis, M., "US/UK Advanced Short Takeoff and Vertical Landing Program," AIAA 89-2039, July 1989.

2. McArdle, J.G. and Smith, C.F., "Flow Studies in Close-Coupled Ventral Nozzles for STOVL Aircraft," SAE paper 901033, Apr. 1990. (See also NASA TM-102554, Apr. 1990.)

3. McArdle, J.G., "Internal Characteristics and Performance of Several Jet Deflectors at Primary-Nozzle Pressure Ratios up to 3.0," NACA TN-4264, June 1958.

4. Raman, G., Zaman, K.B.M.Q., and Rice, E.J., "Initial Turbulence Effect on Jet Evolution With and Without Tonal Excitation." AIAA 87-2725, Oct. 1987.

NASA
National Aeronautics and Space Administration

Report Documentation Page

1. Report No.	2. Government Accession No.	3. Recipient's Catalog No.
NASA TM-103120 AIAA-90-2271		

4. Title and Subtitle

Performance Characteristics of a One-Third-Scale, Vectorable Ventral Nozzle for SSTOVL Aircraft

5. Report Date

6. Performing Organization Code

7. Author(s)

Barbara S. Esker and Jack G. McArdle

8. Performing Organization Report No.

E-5448

10. Work Unit No.

505-62-71

9. Performing Organization Name and Address

National Aeronautics and Space Administration
Lewis Research Center
Cleveland, Ohio 44135-3191

11. Contract or Grant No.

13. Type of Report and Period Covered

Technical Memorandum

12. Sponsoring Agency Name and Address

National Aeronautics and Space Administration
Washington, D.C. 20546-0001

14. Sponsoring Agency Code

15. Supplementary Notes

Prepared for the 26th Joint Propulsion Conference cosponsored by the AIAA, ASME, SAE, and ASEE, Orlando, Florida, July 16-18, 1990.

16. Abstract

Several proposed configurations for supersonic short-takeoff, vertical-landing aircraft will require one or more ventral nozzles for lift and pitch control. The swivel nozzle is one possible ventral nozzle configuration. A swivel nozzle (approximately one-third scale) was built and tested on a generic model tailpipe. This nozzle was capable of vectoring the flow up to $\pm 23°$ from the vertical position. Steady-state performance data were obtained at pressure ratios to 4.5, and pitot-pressure surveys of the nozzle exit plane were made. Two configurations were tested: the swivel nozzle with a square contour of the leading edge of the ventral duct inlet, and the same nozzle with a round leading-edge contour. The swivel nozzle showed good performance overall, and the round-leading-edge configuration showed an improvement in performance over the square-leading-edge configuration.

17. Key Words (Suggested by Author(s))	18. Distribution Statement
Performance characteristics Vectorable ventral nozzle SSTOVL	Unclassified – Unlimited Subject Category 01

19. Security Classif. (of this report)	20. Security Classif. (of this page)	21. No. of pages	22. Price*
Unclassified	Unclassified	12	A03

NASA FORM 1626 OCT 86

*For sale by the National Technical Information Service, Springfield, Virginia 22161